ELSEVIER

Chemical Geology 199 (2003) 199–207

CHEMICAL GEOLOGY
INCLUDING
ISOTOPE GEOSCIENCE

www.elsevier.com/locate/chemgeo

Structure of mercury(II)–sulfur complexes by EXAFS spectroscopic measurements

Alistair R. Lennie[a,*], John M. Charnock[a,b], Richard A.D. Pattrick[b]

[a] *CLRC Daresbury Laboratory, Warrington, Cheshire, WA4 4AD, UK*
[b] *Department of Earth Sciences, University of Manchester, Oxford Road, Manchester M13 9PL, UK*

Received 29 July 2002; accepted 13 February 2003

Abstract

We have examined alkaline sulfidic (0.5–0.005 M $NaHS^-$) aqueous solutions of Hg(II)–S complexes [2.8–0.28 mM Hg(II)] using extended X-ray absorption fine structure (EXAFS) and an especially designed spectroscopic cell. The structural environment of Hg in the complex, determined by EXAFS analysis of Hg L_{III} edge fluorescence spectra taken at 298 and 348K, shows Hg coordinated by 2 S atoms at 2.30 Å. Multiple-scattering analysis reveals a linear [–S–Hg–S–] arrangement in the solution complex. These results are consistent with a low coordination number for Hg as predicted by relativistic models, ab initio calculations, and as determined from the structural environment of Hg in crystalline mercury compounds.

Keywords: Complexes; Mercury; Spectroscopic; Sulfide; XAS

1. Introduction

Understanding metal speciation in aqueous solutions is critical for developing models for metal cycling at the surface and within the crust of the Earth. Without such knowledge, the value of thermodynamic and transport modelling of aqueous metals may be restricted, and predictive studies of metal behaviour in aqueous solution thus flawed. At present, there is intense interest in how toxic metals introduced by anthropogenic activities are mobilised or fixed in the biosphere and geosphere. The behaviour of these metals in reducing environments, such as anoxic sediments and soils, is particularly important because such environments act as sinks for many toxic metals. Here, reduced sulfur often controls the transport and deposition of metals; thus understanding metal speciation in solutions in the presence of dissolved sulfide becomes a fundamental starting point for investigations into aqueous toxic metal behaviour.

Mechanisms of transport of Hg in the natural environment are of great interest not only for understanding processes of mineral formation but also because Hg can be a pollutant with harmful physiological effects. Remediation of Hg-contaminated land by chemical treatment is thus an important area of research (Barnett et al., 1997; Biester and Zimmer, 1998, Kim et al., 1999). Our understanding of Hg chemistry in nature has come principally from many studies of geothermal Hg transport and mineralisation or ore formation. Comprehensive reviews of Hg

* Corresponding author. Fax: +44-1925-603-124.
E-mail address: a.lennie@dl.ac.uk (A.R. Lennie).

0009-2541/03/$ - see front matter © 2003 Elsevier Science B.V. All rights reserved.
doi:10.1016/S0009-2541(03)00118-9

speciation and transport in hydrothermal systems are provided by Varekamp and Buseck (1984), Krupp (1988) and Barnes and Seward (1997).

Mercury may be transported in hydrothermal fluids as elemental Hg species in aqueous solution, or in the gas phase. Elemental Hg is also soluble in hydrocarbons. Varekamp and Buseck (1984) have proposed that the abundance of $Hg(0)_{aq}$ is increased by increasing pH, T and by decreasing total S, ionic strength and pO_2. Therefore, under the conditions of geothermal systems, Hg(0) as hexaqua ion or as vapour should be considered as an important species transporting Hg for ore formation. Oxidation of Hg(0) to Hg(II) will lead to HgS precipitation if sulfide is present at concentrations normally found in geothermal systems. Mercury complexes with ligands, such as SO_4^{2-}, Cl^-, OH^- and CO_3^{2-}, do not provide sufficient solubility for Hg(II) transport in sulfide bearing hydrothermal solutions (Krupp, 1988). However, if aqueous solutions are rich in hydrogen sulfide, of neutral to alkaline pH, and at elevated temperature, Hg(II) can be transported as sulfide complexes (Krupp, 1988; Paquette and Helz, 1995).

Recent physicochemical studies of metal solubilities and speciation in sulfidic aqueous media have employed a variety of spectroscopic techniques to elucidate the nature of the solution species. The use of X-ray absorption spectroscopy (XAS) and especially extended X-ray absorption fine structure (EXAFS) is a particularly powerful method for providing local structural information around the atom of interest. Hg L_{III} edge EXAFS has been used to establish the relative proportions of major Hg-bearing phases in mine wastes (Kim et al., 1999) and the mechanism of immobilisation of Hg^{2+} from waste fluids onto goethite (Collins et al., 1999). Surface studies of Hg vapour sorbed on PbS(001) surfaces using XPS and allied techniques show a monolayer of chemisorbed Hg, which is subsequently oxidised to Hg(II); a Hg–S bond length of 2.62 Å with threefold coordination to S was determined (Genin et al., 2001). Hg L_{III} EXAFS studies of $HgCl_2$ dissolved in water or dimethyl sulfoxide show Hg–Cl distances of 2.29(2) Å and 2.31(2) Å, respectively (Åkesson et al., 1994).

In this study, we employ EXAFS to probe the local structural environment of dissolved Hg in the Hg–S complexes present in alkaline solutions at 298 and 348K; a spectroscopic cell was designed and constructed for this purpose. To our knowledge, this is the first study of aqueous Hg–S inorganic complexes using EXAFS.

2. Experimental methodology

2.1. Sample preparation

We prepared mercury sulfide solutions by two different methods. The first method was to form Hg–S complexes by adding $Hg(NO_3)_2{\cdot}H_2O(s)$ to aqueous sulfide (0.5 and 0.05 M) solutions so that there was a slight excess of HgS precipitate. The second method was to dissolve metacinnabar, precipitated from Hg^{2+} and sulfide, in 0.05 M sulfide solution. Metacinnabar was added in excess to provide a solution saturated with Hg–S complexes; these solutions were also diluted by a factor of 10 with deaerated, deionised water for a second cycle of EXAFS data collection upon heating.

All mercury solutions were prepared and stored under nitrogen. Concentrations of dissolved Hg were measured by ICP-AES giving 2.8 mM Hg for the solution formed from metacinnabar dissolved in 0.05 M Na_2S (pH 11.5) and 2.5 mM Hg for mercuric nitrate dissolved in 0.05 M Na_2S (pH 11.3).

2.2. Data collection

Data were obtained at the SRS, CLRC Daresbury Laboratory, UK. The current varied between 150 and 250 mA in the 2 GeV storage ring. Station 16.5 was used to collect the Hg L_{III} edge X-ray fluorescence spectra. This station has been designed as a state of the art facility for ultra dilute EXAFS spectroscopy, with focussing optics to optimise flux at the sample and a high count-rate fluorescence detector. A Si(220) double-crystal monochromator is employed, and the second crystal can be dynamically bent during scanning to achieve horizontal focus.

The monochromator was calibrated with $Hg(NO_3)_2{\cdot}H_2O(s)$, the edge of which was measured as 12,283 eV. The X-ray adsorption data for the solid was collected in transmission mode using ion chambers filled with Ar and He so as to absorb 20% of the incident monochromatic beam at the Hg edge in the first ion chamber and 80% in the second ion chamber.

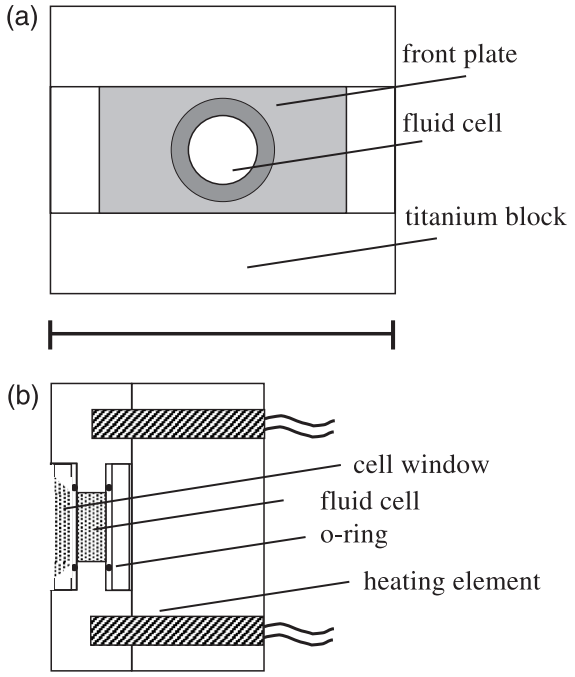

Fig. 1. Schematic illustration of the solution cell used for Hg L_{III} edge X-ray fluorescence measurements. (a) Front view of cell. (b) Side view of cell showing cell position at front and cartridge heater location in the supporting block. The titanium cell has 0.125 mm PEEK windows and Viton® o-ring seals. Cartridge heaters powered by a Eurotherm-controlled power supply are used to maintain set temperatures to within ± 1 K. A K-type thermocouple located in the supporting block provides the temperature signal for the control circuit. The scale bar is 60 mm.

Fluorescence data were obtained from the solutions using a spectroscopic cell developed for these experiments. The titanium cell, with 0.125 mm PEEK windows, is backed with a titanium block containing cartridge heaters to allow internal heating (Fig. 1). Thermostatic control is achieved using a Eurotherm heating controller. The control thermocouple is located close to the cell fluid chamber to maintain the temperature within ± 1 K of the desired temperature. Solutions containing mercury sulfide complexes were loaded into the cell under nitrogen. For X-ray fluorescence measurements, the cell was mounted with the front window angled at 45° to the incident X-ray beam.

Solution data were collected in fluorescence mode, with measurements taken at 90° to the beam direction in plane position. The Ortec 30-element fluorescence detector is a high-purity Ge solid-state detector array coupled to high count-rate electronics. Count rates in excess of 200 kHz per channel are achieved without loss of linearity. The front of the detector was located 6 cm from the cell window. For these measurements, between four and eight spectra were recorded and averaged for each sample to improve the EXAFS signal-to-noise ratio. Spectra were collected from sulfidic solutions into which either mercuric nitrate or metacinnabar were dissolved, as described above. Individual spectra to $k = 14$ Å^{-1} were collected in about 40 min at 298 and 348K; the dynamic focusing was only employed on the most dilute solution.

2.3. Data processing

The Hg L_{III} edge spectra were calibrated in the SRS program EXCALIB. The edge position of each spectrum was determined as being the maximum in the first derivative of the fluorescence signal. Data were background subtracted using the SRS program EXBACK. EXAFS data analyses were performed using curved wave theory in the program EXCURV98 (Binsted, 1998; Gurman et al., 1984; Gurman et al., 1986). Phaseshifts were calculated ab initio using Hedin–Lundqvist exchange potentials and von Barth ground-state potentials. For each spectrum, the parameters refined were E_f, an energy offset, and for each shell, the distance from the central Hg, and a Debye–Waller

Table 1
EXAFS analyses of Hg solution complexes obtained by X-ray fluorescence on Station 16.5, Daresbury Laboratory

Sample (T, K)	Scatterer	N	r (Å)	$2\sigma^2$ (Å^2)	R
$Hg(NO_3)_2$ + 0.5 M Na_2S (298 K)	S	2	2.31	0.006	26.6
[*Multiple scattering fit*]	S	2	2.31	0.006	24.8
$Hg(NO_3)_2$ + 0.05 M Na_2S (298 K)	S	2	2.30	0.005	25.4
[*Multiple scattering fit*]	S	2	2.30	0.006	23.2
$Hg(NO_3)_2$ + 0.05 M Na_2S (348 K)	O	1	2.20	0.006	37.5
	S	1	2.30	0.006	

The Hg L_{III} edge position was measured at 12284 eV. The samples were prepared by dissolving $Hg(NO_3)_2 \cdot H_2O$ in 0.5 or 0.05 M Na_2S solutions.
N is the number of scatterers in the shell ± 25%; r is the absorber–scatterer distance ± 0.02 Å; $2\sigma^2$ is the Debye–Waller factor ± 25%; R is a least-squared residual, showing the goodness of fit.

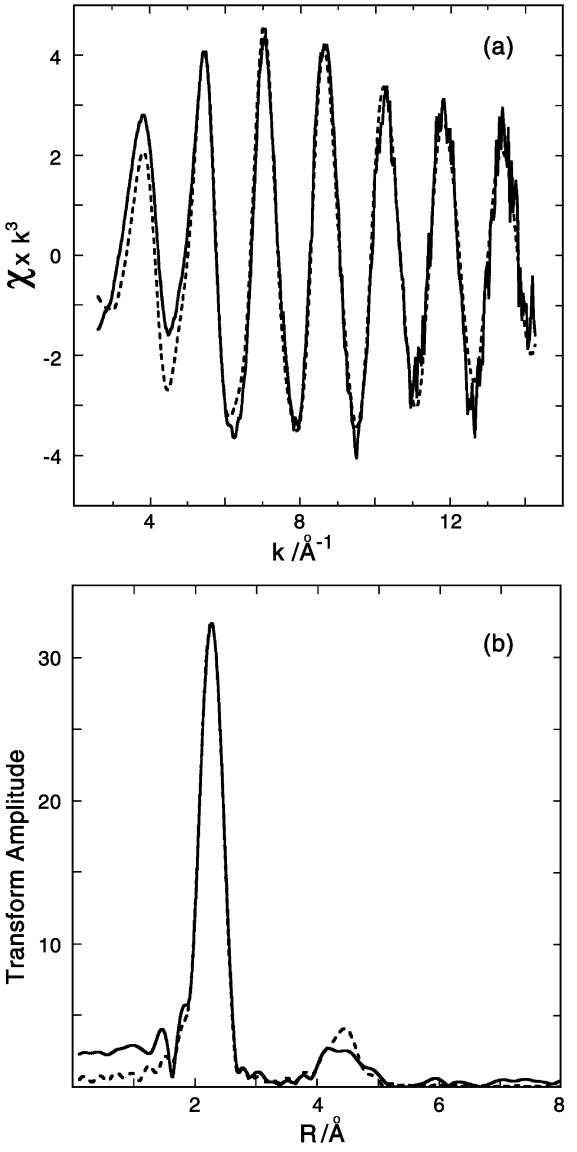

Fig. 2. (a) Experimental Hg L_{III} edge EXAFS spectrum (solid line) and theoretical fit (broken line) of the Hg–S solution complex formed at 298 K by reaction of $Hg(NO_3)_2 \cdot H_2O$ with 0.05 M Na_2S (eight scans). (b) Fourier transform (sulfur phase-shift corrected) of the spectrum (solid line) and fit (broken line).

factor which represents both static and thermal disorder. The fit index, R, is defined in Binsted et al. (1992). For each spectrum, several models for the shell surrounding the central Hg atom were tested. These included 2 S, 1 S and 1 O, 2 S and 1 O, and 3 S.

Although the presence of a mixture of species in solution may give an average noninteger coordination, in order to model any multiple scattering, it is necessary to define a model with a set geometry and set coordination numbers for each species present. To minimise

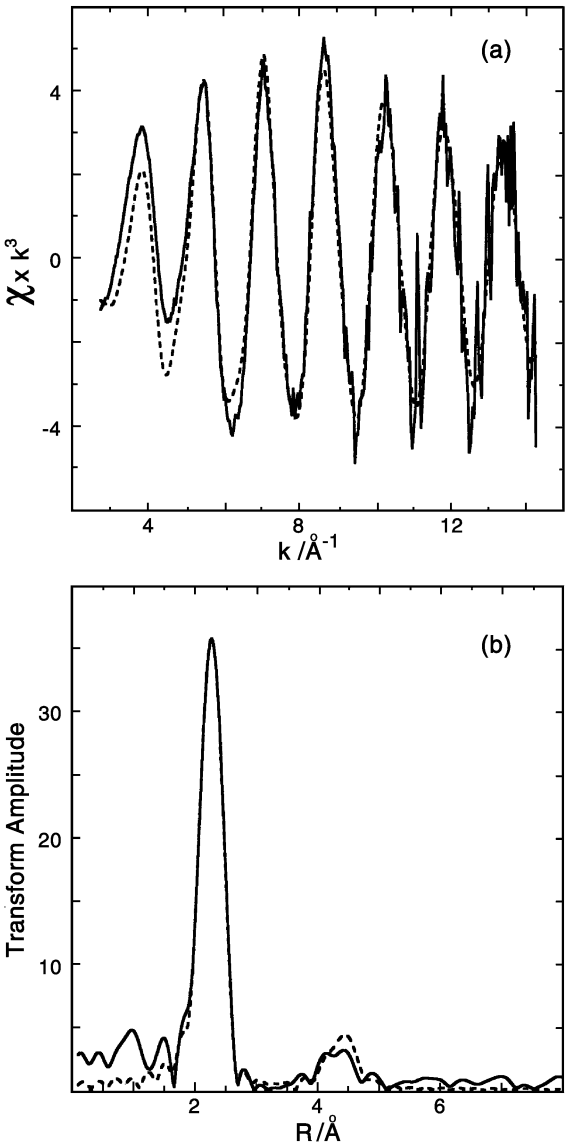

Fig. 3. (a) Experimental Hg L_{III} edge EXAFS spectrum (solid line) and theoretical fit (broken line) of the Hg–S solution complex formed at 298 K by reaction of HgS with 0.05 M Na_2S (eight scans). (b) Fourier transform (sulfur phase-shift corrected) of the spectrum (solid line) and fit (broken line).

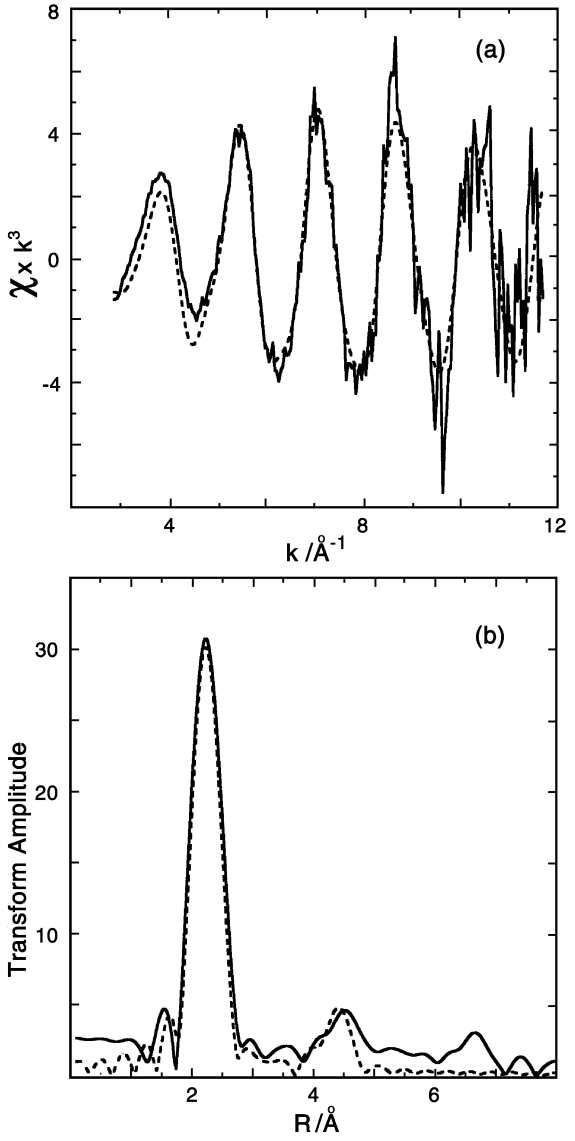

Fig. 4. (a) Dynamically focussed experimental Hg L_{III} edge EXAFS spectrum (solid line) and theoretical fit (broken line) of the Hg–S solution complex formed at 298 K by reaction of HgS with 0.05 M Na_2S and diluted by a factor of 10 (eight scans). (b) Fourier transform (sulfur phase-shift corrected) of the spectrum (solid line) and fit (broken line).

the number of variable parameters used in the multiple-scattering fits, we assumed that one major species would be present; therefore, the number of atoms in each shell was chosen as the integer value which gave the best fit (lowest R value).

3. Results

Analyses of the EXAFS data are summarised in Tables 1 and 2. Hg-EXAFS data collected at 298K from the solution prepared by addition of $Hg(NO_3)_2{\cdot}H_2O$ to 0.5 M Na_2S are fitted with 2 S coordinating the Hg at 2.31 Å. The fit to the EXAFS was improved by including multiple-scattering contributions assuming a linear S–Hg–S geometry. The same result was found for EXAFS of the Hg solution prepared by addition of $Hg(NO_3)_2{\cdot}H_2O$ to 0.05 M Na_2S. Inclusion of multiple scattering again significantly improved the fit. This can be seen in the Fourier transform by the fitting of a peak at ~ 4.6 Å (Fig. 2). Upon heating this sample to 348 K, the EXAFS fit shows a change in structure of the Hg complex. Here, the best fit to the data is coordination by 1 S at 2.29 Å and 1 O at 2.20 Å, which gives a significant improvement in fit compared with fitting the data with 2 S coordinating Hg. In this case, there is no significant multiple-scattering contribution to the EXAFS.

EXAFS data of the second set of Hg solutions, formed by dissolving HgS (metacinnabar) in 0.05 M Na_2S, were collected at 298 K (Fig. 3) and 348 K and fitted with 2 S coordinating Hg at 2.30 Å in both cases. Data collection on the diluted solution containing 0.005 M Na_2S and ~ 0.28 mM Hg used the dynamic focussing of the second monochromator which improved the signal-to-noise ratio by a factor of 10 (Fig. 4). At 298 and 348 K, the EXAFS data from 0.005 M Na_2S solutions are fitted with 2 S coordinating Hg at 2.30

Table 2
EXAFS analyses of Hg solution complexes obtained by X-ray fluorescence on Station 16.5, Daresbury Laboratory

Sample (T, K)	Scatterer	N	r (Å)	$2\sigma^2$ (Å^2)	R
HgS in 0.05 M Na_2S (298 K)	S	2	2.30	0.004	32.2
[*Multiple scattering fit*]	S	2	2.30	0.005	30.7
HgS in 0.05 M Na_2S (348 K)	S	2	2.30	0.005	30.5
[*Multiple scattering fit*]	S	2	2.30	0.005	27.8
HgS in 0.05 M Na_2S (298 K)[a]	S	2	2.30	0.005	39.5
[*Multiple scattering fit*]	S	2	2.30	0.005	36.4
HgS in 0.05 M Na_2S (348 K)[a]	S	2	2.28	0.007	44.8
[*Multiple scattering fit*]	S	2	2.28	0.007	42.9

The Hg L_{III} edge position was measured at 12284 eV. The samples were prepared by dissolving HgS in 0.05 M Na_2S solution.
N is the number of scatterers in the shell ± 25%; r is the absorber–scatterer distance ± 0.02 Å; $2\sigma^2$ is the Debye–Waller factor ± 25%; R is a least-squared residual, showing the goodness of fit.
[a] Diluted by a factor of 10 and focussed.

and 2.28 Å, respectively. A number of oxygen plus sulfur combinations were tested but did not improve the fit to the EXAFS. Inclusion of multiple scattering from a linear geometry significantly improved the fit to the EXAFS in all four samples (Table 2). There is no evidence for a hydration shell around Hg in the samples measured at 298 K.

4. Discussion

4.1. A two-coordinate linear complex

The results from our experiments show that Hg in high pH sulfidic solutions is two coordinate with sulfur, with Hg–S bond distances in the range 2.29 ± 0.02 Å. Furthermore, significant improvements to the EXAFS fit are achieved when multiple scattering is employed, assuming a linear geometry. Multiple scattering is characteristic of linear homoleptic moieties X–M–X (van der Gaauw et al., 1999) and is due to scattering pathways which may include the central absorber as well as the ligand atoms. This results in a contribution to the EXAFS which is manifested in the Fourier transform as a peak at circa twice the absorber–scatterer distance (in this case, ~ 4.6 Å). The observance of this contribution (Tables 1 and 2, Figs. 2–4) provides strong evidence that the Hg coordinated by 2 S adopts a linear structure within the solution complex.

4.2. Hg–S bond distances

The Hg–S bond distances of ~ 2.29 Å in the complexes measured in this study are comparable to those found in cinnabar (HgS), which has Hg–S distances of 2.368 Å in the –S–Hg–S–Hg– infinite chains running through the structure. Here, the –S–Hg–S– bond angle within the linear chains is 172.7°; each Hg atom is coordinated by an additional 4 S atoms located in adjacent chains at distances of 3.094 Å (2 S) and 3.287 Å (2 S) (Auvray and Genet, 1973), resulting in sixfold coordination. In contrast, metacinnabar (HgS, with the sphalerite structure) has Hg coordinated by 4 S at 2.534 Å (Aurivillius, 1964, 1965). The crystal structure of $Na_2Hg_3S_4{\cdot}(H_2O)_2$(s) shows Hg in both twofold and fourfold coordination with Hg–S distances of 2.362 and 2.558 Å, respectively (Banda et al., 1991). Hence, Hg–S distances obtained from our data are consistent with those for Hg in twofold coordination with S in solids.

4.3. Linear twofold coordination in Hg chemistry

Linear twofold coordination is common in Hg chemistry. In general, Hg(II) compounds are formed with either two collinear or four tetrahedral bonds. A feature of many of the crystals with two collinear bonds is four more distant neighbours, described as characteristic and effective coordinate numbers, respectively, and forming a distorted (2 + 4) octahedral group. For example, HgX_2, where X = Cl, Br, or I (yellow form), crystallise as linear molecules X–Hg–X, with four halogens from other X–Hg–X molecules giving the distorted octahedral coordination referred to above. These HgX_2 linear molecules are also present in the vapour state. The small coordination numbers observed in Hg compounds are a consequence of relativistic effects (Kaupp and von Schnering, 1994; Pyykko, 1988; Tossell and Vaughan, 1981).

4.4. Hg (bi)sulfide complexes

The high solubility of Hg as HgS complexes in solutions within the stability field of cinnabar in high concentrations of reduced S and neutral to alkaline pH is well known (Krupp, 1988; Schwarzenbach and Widmer, 1963). A number of Hg–S solution species have been proposed to account for this solubility. Schwarzenbach and Widmer (1963) proposed the (pH dependent) species $Hg(HS)_2$, $HgS(HS)^-$ and HgS_2^{2-}. In contrast, Barnes et al. (1967) proposed four possible complexes, $HgS(H_2S)_2$, $Hg(HS)_3^-$, $HgS(HS)_2^{2-}$ and HgS_2^{2-}, to model results from experiments in which Hg(II) was dissolved in 2.5 M sulfide solutions. According to Barnes (1979), $Hg(HS)_2$ is the dominant species at pHs less than 6, $HgS(HS)^-$ between pH = 6 and 8, and HgS_2^{2-} above pH = 8; $HgS(HS)(OH)^{2-}$ requires high pHs which are outside the pH range of natural waters.

The only spectroscopic measurement of Hg–S complexes in aqueous solution prior to our experiment was a Raman study (Cooney and Hall, 1966) from which the Raman spectrum was used to assign the $[-S-Hg-S-]^{2-}$ complex to the linear point group $D_{\infty h}$. One consistency of these previous studies is the

proposed presence of an HgS_2^{2-} species at high pH. The two-coordinate linear species identified in our experiments is also consistent with HgS_2^{2-} (as $[S-Hg-S]^{2-}$). EXAFS cannot be used to distinguish between the species $Hg(HS)_2$, $HgS(HS)^-$ and HgS_2^{2-}.

Using ab initio quantum mechanical methods, Tossell (1999, 2001) has calculated a number of structures for Hg–S complexes in which Hg is two-coordinate (Table 3). The molecule HS–Hg–S–Hg–SH has a calculated ⟨S–Hg–S⟩ angle of 179°. Calculated Hg–S distances in these molecular species generally seem to provide an overestimate of Hg–S distances when compared with our experimental results. However, there are at present no ab initio quantum mechanical calculations for an $[S-Hg-S]^{2-}$ solution species.

Paquette and Helz (1997) present pH-dependent distributions for aqueous mercuric sulfide complexes which indicate that above pH = 11, HgS_2^{2-} is the predominant species in solutions either saturated with, or containing negligible, zero-valent sulfur. Both thiol and sulfide ligands favour formation of stable complexes with Hg(II), decomposing polyatomic Hg cations, and oxidising Hg(0). It is extremely unlikely therefore that mercury speciation is anything other than Hg(II) under the conditions of our experiment. Mercuric polysulfides are proposed as the species giving enhanced Hg solubility in S(0)-saturated solutions up to pH = 9.5. This enhancement is expected to decrease relative to the solubility of mercury-reduced sulfur species at higher pHs, with HgS_2^{2-} remaining the predominant mercury–sulfur species under these conditions (Paquette and Helz, 1997). Our EXAFS results are consistent with mercury speciation in sulfidic solutions at high pH discussed by Paquette and Helz (1997).

Table 3
Hg–S and Hg–O bond lengths in thio- [oxo-] Hg species (Tossell, 1999, 2001)

Molecule	r (Hg–S) [Å]	r (Hg–O) [Å]
$Hg_2S(SH)_2$	2.39 (HF)	
	2.36 (MP2)	
HgS	2.362 (HF)	
	2.273 (MP2)	
	2.317 (QCISD)	
H_2O–Hg–S	2.296 (HF)	2.457 (HF)
	2.244 (MP2)	2.357 (MP2)
	2.274 (QCISD)	2.399 (QCISD)
HO–Hg–SH	2.373 (HF)	2.010 (HF)
	2.350 (MP2)	2.015 (MP2)
	2.365 (QCISD)	2.021 (QCISD)

Hg–S and Hg–O distances were derived from ab initio calculations as reported by Tossell (1999, 2001).
HF: Hartree Fock; MP2: Moller–Plesset many-body perturbation theory; QCISD: Quadratic configuration interaction with single and double substitutions.

4.5. Hydrolysis of solution complex

The Hg-EXAFS of the solution prepared with mercuric nitrate and heated to 348 K was significantly different to the other solutions and was fitted with 1 S and 1 O in the inner coordination sphere. Although the fit was not improved by inclusion of multiple-scattering effects, this does not rule out a linear geometry because the Hg–O and Hg–S distances and the scattering properties of O and S are different, which would tend to smear out any multiple-scattering effects. However, the presence of oxygen suggests partial hydrolysis of the $[-S-Hg-S-]^{2-}$ complexes by nitrate, consistent with the observations of Banda et al. (1989). Although we have not identified this solution species, potential candidates come from calculations of Hg–(S,O) aqueous species Hg(SH)(OH) or $Hg(S)H_2O$ (Tossell, 2001). However, it is not possible from comparisons of Hg–O calculated distances (Table 3) with our experimental Hg–O distance (Table 1) to identify the coordinating oxygen as belonging to either H_2O or OH^-.

4.6. Formation of HgS minerals from Hg^{2+} and HS^-

There is now some evidence indicating how HgS minerals form from hydrothermal systems. HgS crystallises in nature in two forms, cinnabar and metacinnabar, the latter being thermodynamically unstable below 344 °C (Barnes and Seward, 1997). An earlier Hg-EXAFS study of the formation of Hg–S precipitates (Pattrick et al., 1999) revealed that in the first 2 s after precipitation, a low coordination number (1) and short bond length (2.36 Å) Hg–S species formed, followed by a rapid attainment of fourfold coordination of Hg by S, with an Hg–S distance of 2.53 Å. Here, it appears that the structure of the first formed solid is related to the HgS_2^{2-} solution species in the present experiment. Kinetic factors then favour development of fourfold S coordinate (metastable) meta-

cinnabarlike structure rather than a sixfold S coordinate cinnabarlike structure. Similar kinetic behaviour is observed with iron and copper sulfide formation, where metastable low-temperature, low-coordinate phases form on precipitation of sulfide ions with the relevant metal cation (Lennie and Vaughan, 1996; Pattrick et al., 1997). However, exact mechanisms of HgS precipitation from Hg–S solution complexes remain to be fully established.

5. Conclusion

We have successfully established the performance of the spectroscopic cell on Station 16.5 at the SRS Daresbury for use in low-concentration EXAFS experiments. Using the horizontal focussing facility on the second monochromator, high-quality data were produced by summing eight scans of a sample containing ~ 0.28 mM Hg in 0.005 M sulfide (Fig. 4). Analysis of EXAFS has provided direct structural evidence for the existence of twofold linear Hg–S complexes in high pH, sulfidic solutions.

This study has focussed on high pH solutions with relatively high dissolved Hg concentrations. One intriguing future experiment would be to use EXAFS to test the observation that cinnabar solubility is increased in solutions containing both S(0) and HS^- relative to those containing HS^- alone (Paquette and Helz, 1997). Paquette and Helz (1997) have proposed that S(0) increases cinnabar solubility in sulfidic sediments by formation of bidentate polysulfide ligands, i.e.

$$HgS(cinn) + SH^- + (n-1)S(0) = Hg(S_n)SH^-$$

which suggests that Hg is coordinated by 3 S. Tossell (1999) has modelled this proposed species as $Hg(S_4)(SH)^{-1}$ with Hg coordinated by 3 S, two from an S_4^{2-} polysulfide and one from SH^{-1}. Calculated enhancement of cinnabar dissolution by S_8 exceeds that measured by Paquette and Helz (1997) by a factor of 10^5.

Developing the Paquette and Helz (1997) model, Jay et al. (2000) have proposed that $Hg(S_x)_2^{2-}$, where Hg is four coordinated by S, dominates speciation of Hg(II) in high pH waters, where both S(0) and HgS(s) are present. Our experiments have shown no evidence for Hg in either three or four coordination with S. Thus, as yet, there is no spectroscopic evidence for Hg coordinated by 4 S in aqueous solution although four-coordinate Hg–S is found in complexes synthesised in DMF (Bailey et al., 1991) with bond distances at 2.540(2) Å. EXAFS would be the technique of choice for investigating the presence of these proposed species in the presence of S(0) and, if present, both longer bond lengths and larger coordination numbers than those observed in our experiments may be expected.

It is also clear that further improvements in flux to the fluorescence detector from dilute solutions of Hg–S complexes are achievable by optimising both cell and detector geometries. This would enable EXAFS data to be collected from solutions an order of magnitude more dilute than the most dilute in this study, allowing spectroscopic measurements of Hg coordination by S in solutions of pH 10 or less (Paquette and Helz, 1997; Jay et al., 2000). These would then be of direct relevance to conditions found in the natural environment.

Acknowledgements

We are grateful to NERC for a ROPA award (GR3/R9926). We thank Barry Gale for construction of the cell and wish to acknowledge Bob Bilsborrow, Fred Mosselmans, the Director and staff of the SRS for their help during our experiments at the Daresbury Laboratory. **[EO]**

References

Åkesson, R., Persson, I., Sandström, M., Wahlgren, U., 1994. Structure and bonding of solvated mercury (II) and thallium (III) dihalide and dicyanide complexes by XAFS spectroscopic measurements and theoretical calculations. Inorg. Chem. 33, 3715–3723.

Aurivillius, K., 1964. An X-ray and neutron diffraction study of metacinnabarite. Acta Chem. Scand. 18, 1552–1553.

Aurivillius, K., 1965. Correction to "An X-ray and neutron diffraction study of metacinnabarite". Acta Chem. Scand. 19, 522.

Auvray, P., Genet, F., 1973. Affinement de la structure cristalline du cinabre α-HgS. Bull. Soc. Fr. Mineral. Cristallogr. 96, 218–219.

Bailey, T.D., Banda, R.M.H., Craig, D.C., Dance, I.G., Ma, I.N.L., Scudder, M.L., 1991. Mercury polysulfide com-

plexes, $[Hg(S_x)(S_y)]^{2-}$: syntheses, ^{199}Hg NMR studies in solution, and crystal structure of $(Ph_4P)_4[Hg(S_4)_2]Br_2$. Inorg. Chem. 30, 187–191.

Banda, R.M.H., Dance, I.G., Bailey, T.D., Craig, D.C., Scudder, M.L., 1989. Cadmium polysulfide complexes, $[Cd(S_x)(S_y)]^{2-}$—syntheses, crystal and molecular-structures, and Cd-113 NMR-studies. Inorg. Chem. 28, 1862–1871.

Banda, R.M.H., Craig, D., Dance, I.G., Scudder, M., 1991. Tetrahedral HgS_4 and linear HgS_2 coordination in the crystal structure of $Na_2Hg_3S_4(H_2O)_2$. Polyhedron 10, 41–45.

Barnes, H.L., 1979. Solubilities of ore minerals. In: Barnes, H.L. (Ed.), Geochemistry of Hydrothermal Ore Deposits, 2nd ed. Wiley, New York, pp. 404–460.

Barnes, H.L., Seward, T.M., 1997. Geothermal Systems and Mercury Deposits Chapter 14. In: Barnes, H.L. (Ed.), Geochemistry of Hydrothermal Ore Deposits, 3rd ed. Wiley.

Barnes, H.L., Romberger, S.N., Stembrok, M., 1967. Ore solution chemistry: II. Solubility of HgS in sulfide solutions. Econ. Geol. 62, 957–982.

Barnett, M.O., Harris, L.A., Turner, R.R., Stevenson, R.J., Henson, T.J., Melton, R.C., Hoffman, D.P., 1997. Formation of mercuric sulfide in soil. Environ. Sci. Technol. 31, 3037–3043.

Biester, H., Zimmer, H., 1998. Solubility and changes of mercury binding forms in contaminated soils after immobilization treatment. Environ. Sci. Technol. 32, 2755–2762.

Binsted, N., 1998. EXCURV98. CCLRC Daresbury Laboratory Computer Program.

Binsted, N., Strange, R.W., Hasnain, S.S., 1992. Constrained and restrained refinement in EXAFS data analysis with curved wave theory. Biochemistry 31, 12117–12125.

Collins, C.R., Sherman, D.M., Ragnarsdottir, K.V., 1999. Surface complexation of Hg^{2+} on goethite: mechanism from EXAFS spectroscopy and density functional calculations. J. Colloid Interface Sci. 219, 345–350.

Cooney, R.P.J., Hall, J.R., 1966. Raman spectrum of thiomercurate(II) ion. Aust. J. Chem. 19, 2179–2180.

Genin, F., Alnot, M., Ehrhardt, J.J., 2001. Interaction of vapours of mercury with PbS(001): a study by X-ray photoelectron spectroscopy, RHEED and X-ray absorption spectroscopy. Appl. Surf. Sci. 173, 44–53.

Gurman, S.J., Binsted, N., Ross, I., 1984. A rapid, exact, curved-wave theory for EXAFS calculations. J. Phys. C 17, 143–151.

Gurman, S.J., Binsted, N., Ross, I., 1986. A rapid, exact, curved-wave theory for EXAFS calculations: 2. The multiple-scattering contributions. J. Phys. C 19, 1845–1861.

Jay, J.A., Morel, F.M.M., Hemond, H.F., 2000. Mercury speciation in the presence of polysulfides. Environ. Sci. Technol. 34, 2196–2200.

Kaupp, M., von Schnering, H.G., 1994. Dominance of linear 2-coordination in mercury chemistry: quasirelativistic and nonrelativistic ab initio pseudopotential study of $(HgX_2)_2$ (X = F, Cl, Br, I, H). Inorg. Chem. 33, 2555–2564.

Kim, C.S., Rytuba, J.J., Brown Jr., G.E., 1999. Utility of EXAFS in characterization and speciation of mercury-bearing mine wastes. J. Synchrotron Radiat. 6, 648–650.

Krupp, R.E., 1988. Physicochemical aspects of mercury metallogenesis. Chem. Geol. 69, 345–356.

Lennie, A.R., Vaughan, D.J., 1996. Spectroscopic studies of iron sulfide formation and phase relations at low temperatures. Mineral Spectroscopy: A Tribute to Roger G. Burns, The Geochemical Society, Special Publication No. 5, pp. 117–131.

Paquette, K., Helz, G., 1995. Solubility of cinnabar (red HgS) and implications for mercury speciation in sulfidic waters. Water Air Soil Pollut. 80, 1053–1056.

Paquette, K., Helz, G., 1997. Inorganic speciation of mercury in sulfidic waters: the importance of zero-valent sulfur. Environ. Sci. Technol. 31, 2148–2153.

Pattrick, R.A.D., Mosselmans, J.F.W., Charnock, J.M., England, K.E.R., Helz, G.R., Garner, C.D., Vaughan, D.J., 1997. The structure of amorphous copper sulfide precipitates: an X-ray absorption study. Geochim. Cosmochim. Acta 61, 2023–2036.

Pattrick, R.A.D., Charnock, J.M., Mosselmans, J.F.W., 1999. Structural development of HgS precipitated from aqueous solution; determined by XAS. CLRC, Synchrotron Radiation Department Annual Report, 1998–1999. Annex, pp. 90–91.

Pyykko, P., 1988. Relativistic effects in structural chemistry. Chem. Rev. 88, 563–594.

Schwarzenbach, G., Widmer, M., 1963. Die Löslichkeit von Metallsulfiden: I. Schwarzes Quecksilbersulfid. Helv. Chim. Acta 46, 2613–2628.

Tossell, J.A., 1999. Theoretical studies on the formation of mercury complexes in solution and the dissolution and reactions of cinnabar. Am. Mineral. 84, 877–883.

Tossell, J.A., 2001. Calculation of the structures, stabilities, and properties of mercury sulfide species in aqueous solution. J. Phys. Chem., A 105, 935–941.

Tossell, J.A., Vaughan, D.J., 1981. Relationships between valence orbital binding energies and crystal structures in compounds of copper, silver, gold, zinc, cadmium and mercury. Inorg. Chem. 20, 3333–3340.

van der Gaauw, A., Wilkin, O.M., Young, N.A., 1999. The importance of multiple scattering pathways involving the absorbing atom in the interpretation and analysis of metal K-edge XAFS data of co-ordination compounds. J. Chem. Soc. Dalton Trans., 2405–2406.

Varekamp, J.C., Buseck, P.R., 1984. The speciation of mercury in hydrothermal systems, with applications to ore deposition. Geochim. Cosmochim. Acta 48, 177–185.